



① I-13980

PPPL-2087  
DR-2207-1

ON THE MURAKAMI DENSITY LIMIT IN  
TOKAMAKS AND REVERSED-FIELD PINCHES

By

F.W. Perkins and R.A. Hulse

MARCH 1984

MAILED

PLASMA  
PHYSICS  
LABORATORY **PPPL**

ON THE MURAKAMI DENSITY LIMIT IN  
TOKAMAKS AND REVERSED-FIELD PINCHES

F. W. Perkins and R. A. Hulse

Plasma Physics Laboratory, Princeton University  
Princeton, New Jersey 08544

PPPL--2087

DP84 009353

ABSTRACT

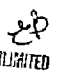
A theoretical upper limit for the density in an ohmically heated tokamak discharge follows from the requirement that the ohmic heating power deposited in the central current-carrying channel exceed the impurity radiative cooling in this critical region. A compact summary of our results gives this limit  $n_M$  for the central density as

$$n_M = [Z_e/(Z_e-1)]^{1/2} n_{eo} (B_T/1T)(1m/R)$$

where  $n_{eo}$  depends strongly on the impurity species and is remarkably independent of the central electron temperature  $T_e(0)$ . For  $T_e(0) \sim 1$  keV, we have  $n_{eo} = 1.5 \times 10^{14} \text{ cm}^{-3}$  for beryllium,  $n_{eo} = 5 \times 10^{13} \text{ cm}^{-3}$  for oxygen,  $n_{eo} = 1.0 \times 10^{13} \text{ cm}^{-3}$  for iron, and  $n_{eo} = 0.5 \times 10^{13} \text{ cm}^{-3}$  for tungsten. The results agree quantitatively with Murakami's original observations. A similar density limit, known as the I/N limit, exists for reversed-field pinch devices and this limit has also been evaluated for a variety of impurity species.

DISCLAIMER

This report was prepared as an account of work sponsored by an agency of the United States Government. Neither the United States Government nor any agency thereof, nor any of their employees, makes any warranty, express or implied, or assumes any legal liability or responsibility for the accuracy, completeness, or usefulness of any information, apparatus, product, or process disclosed, or represents that its use would not infringe privately owned rights. Reference herein to any specific commercial product, process, or service by trade name, trademark, manufacturer, or otherwise does not necessarily constitute or imply its endorsement, recommendation, or favoring by the United States Government or any agency thereof. The views and opinions of authors expressed herein do not necessarily state or reflect those of the United States Government or any agency thereof.

DISTRIBUTION OF THIS DOCUMENT IS UNLIMITED 

## 1. INTRODUCTION

In 1976, Murakami et al.<sup>1</sup> reported that the maximum electron density  $\bar{n}_M$  in an ohmically heated tokamak scaled as  $B_T/R$  where  $B_T$  denotes the toroidal magnetic field and  $R$  the major radius. Murakami further noted that  $B_T/R$  was proportional to the central current density. Several papers<sup>2-6</sup> have interpreted this limit as being caused by radiation from partially stripped impurity ions at the edge of the plasma where the local radiative cooling rate is largest. These arguments necessarily involve the electron thermal conductivity at the edge of the plasma - a quantity which is not well-known either theoretically or experimentally. This paper shows that a radiative limiting density results from the simple criterion that the ohmic heating power deposited in the central current-carrying channel exceed the power radiated within the channel by impurity ions. This criterion is independent of models for the electron thermal conductivity, and must be obeyed by all ohmically heated tokamaks.

The Murakami density limit enters prominently into plans for the new generation of large research tokamaks such as TFTR<sup>7</sup> and JET.<sup>8</sup> Because  $B_T/R$  is not large for these devices, the Murakami limit places important constraints on the achievable ohmic plasma densities in these machines. These ohmic plasmas serve as targets for auxiliary heating, and, in the final stages of a tokamak discharge when auxiliary heating has ceased, the Murakami limit also governs the maximum density which allows a disruption-free discharge termination.

The concept of a radiation limit to tokamak densities was explored in the 1976 paper of Gibson.<sup>2</sup> This work relied on empirical formulae to express the magnitude and temperature dependence of energy loss by radiating impurity ions. Since that time, Post et al.<sup>9</sup> have derived expressions for the impurity

radiative cooling rates using coronal equilibrium theory. The paper of Ashby and Hughes<sup>4</sup> used these expressions to obtain a formula for a density limit in tokamaks. The Ashby-Hughes formula follows from the statement that the ohmic heating power deposited in the central plasma must exceed the power radiated by the plasma periphery. Clearly, all steady-state plasmas must satisfy this condition, but the resulting formula for the density limit involves the electron thermal conductivity in the plasma periphery which is not well-known. Our arguments indicate that a tokamak discharge can often meet this peripheral boundary condition via the freedom to adopt a particular central electron temperature provided the electron thermal diffusivity in the edge plasma remains below the Bohm value. Recent papers by Roberts<sup>6</sup> also concentrate on the edge plasma and assume an empirical formula for the electron thermal conductivity in the plasma periphery to estimate a density limit.

The aim of this paper is to show that by focusing attention on the central current-carrying portion of the discharge rather than the periphery, one arrives at a useful and straightforward upper limit to the density in ohmically heated tokamaks. The unknown electron thermal conductivity does not enter this argument; only rather general and experimentally well-established properties of the shape of the electron temperature profile are used. Our criterion is simply that no more than 80% of the ohmic heating power deposited within the central current-carrying channel (defined by  $q < 2$ ) can be radiated within this channel by impurity ion cooling. For common impurity species, this density limit is found to be insensitive to the central electron temperature  $T_0$  for experimentally typical values. The density limit exhibits a strong dependence on the impurity species. This simple density limit applies to all ohmically heated tokamak discharges, regardless of size or

thermal conductivity physics. In particular, it will govern the density range where large tokamaks such as TFTR and JET can operate disruption-free without auxiliary heating.

Reversed-field pinch devices also rely on ohmic heating to overcome impurity radiation. A high density limit, known as the I/N limit, has been identified and shown to agree with impurity radiation losses.<sup>10</sup> The contribution of this paper is to evaluate a radiative I/N limit for a variety of impurity elements.

Section 2 presents our principal arguments and results. Application to the I/N limit of reversed-field pinches is presented in Sec. 3. The paper concludes with a discussion.

## 2. TOKAMAK DENSITY LIMIT

The goal of this section is to derive a formula relating our limiting central density in an ohmically heated tokamak to the expression for coronal equilibrium radiative cooling rates. Evaluation of these cooling rates for many atomic species permits us to compute the limiting density as a function of central electron temperature and impurity species. Because this limiting density turns out to be remarkably independent of central temperature, we can define a limiting density for each impurity species. It also becomes independent of impurity concentration when the effective charge  $Z_e \gg 1$ .

The starting point for our calculations is an empirical model that describes the central current-carrying portion of a tokamak discharge. Our model assumes: (1) a Gaussian temperature profile, (2)  $q = 1$  on the magnetic axis, (3) a uniform concentration of impurity ions, (4) a single impurity species, and (5) a coronal equilibrium model for impurity ionization states and radiation rates. Our limiting density then follows from the criterion

that the radiative losses cannot exceed 80% of the ohmic heating power input within the  $q < 2$  current-carrying channel where most of the ohmic heating power is deposited.

A Gaussian temperature profile is quite representative of experimental results in the central current-carrying portion of a tokamak discharge.<sup>11,12</sup> We shall use this model only in regions where  $q < 2$  (i.e., where  $T_e/T_0 \geq 0.3$ ). Consequently, our results will not be sensitive to the rapid decrease of the Gaussian at large radii. This rapid decrease is an artifact of the Gaussian functional form rather than of physics results. The statement that  $q = 1$  on the magnetic axis simply serves to relate the central current density to the toroidal field and major radius. The assumption of a constant impurity concentration across the plasma radius is consistent with experimental data from typical plasma discharges<sup>13</sup> and could follow from mixing by turbulent  $\mathbf{E} \times \mathbf{B}$  velocities of drift waves which transport various ionization stages without regard for their charge state.

All tokamak discharges must supply a sufficient heat flux to the edge region where atomic radiative cooling rates are the largest.<sup>3,4</sup> Since the ohmic heating rate in the current-carrying channel varies as  $T_0^{-3/2}$ , an ohmically heated tokamak discharge may accommodate this demand by adopting a particular value for  $T_0$ . Looking forward to our results, we will find them to be insensitive to  $T_0$ , and hence unaffected by details of the edge power demand. Our maximum density criterion simply requires that a modest fraction (20%) of the  $q < 2$  ohmic heating input be available to maintain the edge plasma, and is insensitive to choice of a smaller fraction.

The integrated heat output  $Q$  of an ohmically heated tokamak discharge can be written as

$$Q(r) \equiv \int_0^r 2\pi r' dr' \left[ \frac{j^2}{\sigma} - \eta n^2 L(T) \right] \quad (1)$$

where

$$\sigma = \sigma_0 \tau^{3/2} / Z_e \quad (2)$$

$$\tau = T_e / T_0 = e^{-r^2/b^2} \quad (3)$$

$$\sigma_0 = \gamma_E^2 \left( \frac{2}{\pi} \right)^{3/2} \frac{(T_0)^{3/2}}{m^{1/2} e^2 (\lambda n \Lambda)} \quad (4)$$

$$Z_e = 1 + \eta \langle Z^2 \rangle \quad (5)$$

Here  $n$  denotes the central electron density,  $\eta$  the relative concentration of impurity ions, and the subscript  $_0$  stands for values at the plasma center. A multi-ionization state reformulation of the average-atom calculations of Post et al.<sup>9</sup> is used for the coronal equilibrium cooling rate  $L(T)$  and the mean square charge state  $\langle Z^2 \rangle$ . These results differ slightly from those tabulated in Ref. 9 as a result of improved energy level screening constants<sup>14</sup> and other modifications. Since this work is concerned with the central regions of a tokamak discharge where the density profile is flat, we shall ignore any difference between the central and local electron densities.

The factor  $\gamma_E$  is tabulated in Spitzer's book.<sup>15</sup> In our work, we shall consider two limits. In the first limit, the impurity concentrations are sufficiently large so that  $Z_e \gg 1$  and  $\gamma_E = 1.00$ . In the second case, the impurities are dilute so that  $Z_e \approx 1$  and  $\gamma_E = 0.582$ . In both cases,  $\gamma_E$  will be constant across the discharge. Interpolation for intermediate cases is straightforward.

In a steady-state tokamak discharge, the current density profile depends on the conductivity and can be written as

$$j = j_0 \sigma / \sigma_0 = j_0 \tau^{3/2} \frac{1 + \eta \langle Z^2 \rangle_0}{1 + \eta \langle Z^2 \rangle}$$

where the central current density  $j_0$  follows from the fact that  $q = 1$  on the magnetic axis

$$j_0 = E_{\text{ext}} c (2\pi R)^{-1} . \quad (6)$$

The Gaussian temperature profile enables us to eliminate the radius in favor of the temperature as the independent variable in the integral (1) for the heat flux.

$$Q(T_0) = \frac{\pi j_0^2 b^2}{\sigma_0} (1 + \eta \langle Z^2 \rangle_0) \int \frac{1}{\tau} \frac{d\tau'}{\tau'} \left[ \tau'^{3/2} \frac{1 + \eta \langle Z^2 \rangle_0}{1 + \eta \langle Z^2 \rangle_{\tau', T_0}} - \Lambda_c \frac{L(\tau', T_0)}{L(\tau_c, T_0)} \right] \quad (7)$$

We introduce here the parameters  $\tau_c$  and  $\Lambda_c$  related by:

$$\Lambda_c = \tau_c^{3/2} \frac{1 + \eta \langle Z^2 \rangle_0}{1 + \eta \langle Z^2 \rangle_{T=\tau_c, T_0}} = \begin{cases} \tau_c^{3/2} & Z_e \approx 1 \\ \tau_c^{3/2} \frac{\langle Z^2 \rangle_0}{\langle Z^2 \rangle_{\tau_c, T_0}} & Z_e \gg 1 \end{cases} \quad (8)$$

while  $\Lambda_c$  in terms of the density is given by

$$\Lambda_c = \frac{\eta r_c^2 L(\tau_c, T_0) (2\pi R)^2 \gamma_E 2(2/\pi)^{3/2} T_e^{3/2}}{B_T^2 c^2 (1 + \eta \langle Z^2 \rangle_0) m^{1/2} e^2 (2n\Lambda)} \quad (9)$$

When expression (8) and (9) for  $\Lambda_c$  are equated, the local ohmic heating input



just balances radiative losses at a temperature  $T = \tau_c T_o$ .

Let us define  $\epsilon$  as the fraction the ohmic heating power input into the region where  $T_e/T_{e0} > \tau$  which is radiated from impurities within this region.

$$\epsilon(T_o, \tau_c) = \begin{cases} \frac{\tau_c^{3/2}}{(2/3)(1-\tau_c^{3/2})} \int_{\tau}^1 \frac{d\tau'}{\tau'} \frac{L(\tau' T_o)}{L(\tau_c T_o)} & z_e \approx 1 \quad (10) \\ \frac{|\tau_c^{3/2} / \langle z^2 \rangle_{\tau_c T_o}| \int_{\tau}^1 \frac{d\tau'}{\tau'} \frac{L(\tau' T_o)}{L(\tau_c T_o)}}{\int_{\tau}^1 \frac{d\tau'(\tau')^{1/2}}{\tau \langle z^2 \rangle_{\tau' T_o}}} & z_e \gg 1 \quad (11) \end{cases}$$

The value of  $\tau$  remains to be specified.

The integrals in Eqs. (10) and (11) run over the central current-carrying portion of a tokamak discharge. We shall define this to be the region where  $1 \leq q \leq 2$ . A posteriori, we will investigate the sensitivity of the limiting density to this definition. Thus, the limit of integration  $\tau$  is defined by  $q = 2$ . The relationship between  $q$  and  $\tau$  can be easily expressed by use of (3)

$$q = \frac{r^2 B_T^c}{2\pi R \int_0^r 2r dr} = \frac{\ln(1/\tau)}{\int_{\tau}^1 \frac{d\tau'(\tau')^{1/2}}{\tau} \left( \frac{1+\eta \langle z^2 \rangle_o}{1+\eta \langle z^2 \rangle_{\tau' T_o}} \right)}. \quad (12)$$

Our two limiting cases yield the simple formulas

$$q(T_0, \tau) = \begin{cases} \frac{3 \ln(1/\tau)}{2(1-\tau^{3/2})} & Z_e = 1 \quad (13) \\ \frac{\ln(1/\tau)}{\int_{\tau}^1 d\tau' (\tau')^{1/2} \frac{\langle Z^2 \rangle_0}{\langle Z^2 \rangle_{\tau' T_0}}} & Z_e \gg 1 \quad (14) \end{cases}$$

The equation  $q(T_0, \tau) = 2$  determines the limit of integration  $\tau$  in (10) and (11). When  $Z_e = 1$ , this limit is  $\tau = 0.346$ . Lastly,  $\tau_c$  is determined by the condition that

$$\epsilon(T_0, \tau_c) = 0.8 \quad (15)$$

The limiting density  $n_c$  is obtained from  $\tau_c$  and  $T_0$  by equating expressions (8) and (9).

$$n_c(T_0) = \frac{B_{T_0} \text{cem}^{1/4} (\ln \Lambda)^{1/2}}{2\pi R} (\text{HF})^{1/2} \quad (16)$$

where

$$H(T_0, \tau_c) = \frac{[\langle Z^2 \rangle_0]^2 \tau_c^{3/2} \pi^{3/2}}{2^{5/2} T_0^{3/2} L(\tau_c T_0) \langle Z^2 \rangle_{\tau_c T_0}} \quad (17)$$

and

$$F = \begin{cases} 1 & Z_e \gg 1 & (18a) \\ \frac{\langle Z^2 \rangle \tau_c T_o}{[\langle Z^2 \rangle_o]^2 \gamma_E \eta} & Z_e \approx 1 & (18b) \end{cases}$$

Equation (18a) expresses the fact that the limiting density is independent of impurity concentration when  $Z_e \gg 1$ . Physically, this occurs because both the impurity radiation and the plasma resistivity (through  $Z_e$ ) are linearly proportional to the impurity concentration.

It remains to express the impurity concentration which enters Eq. (18b) in terms of  $Z_e$  for discharges in which  $Z_e$  is close to unity. The standard experimental determination  $Z_{ex}$  assumes that  $Z_e$  is uniform throughout the plasma cross section, and that the current density scales as  $\tau^{3/2}$ . Under these assumptions, the formula for the plasma resistance  $R_{px}$  is

$$R_{px} = Z_{ex} \frac{2R}{\sigma_o b^2 \int_{\tau_a}^1 \tau^{1/2} d\tau} \equiv \frac{V}{I_p} \quad (19)$$

where  $\tau_a = e^{-a^2/b^2}$  is the value of  $\tau$  at the plasma surface. Here  $V$  denotes the loop voltage,  $I_p$  the plasma current, and  $Z_{ex}$  the experimental value for  $Z_e$  determined by combining the experimental values of  $V$ ,  $I_p$ , and  $T_e(r)$  according to Eq. (19).

Our model assumes that the impurity ion concentration, not  $Z_e$ , is uniform throughout the plasma cross section. The plasma current is then

$$I_p = j_0 (1 + \eta \langle Z_0^2 \rangle) b^2 \pi \int_{\tau_a}^1 \frac{\tau^{1/2} d\tau}{(1 + \eta \langle Z^2 \rangle)} \quad (20)$$

The loop voltage is evaluated on the magnetic axis by

$$V = \frac{j_0 2\pi R}{\sigma_0} (1 + \eta \langle Z^2 \rangle_0) \quad (21)$$

Combining Eqs. (19) - (21) yields the desired relation between  $Z_{ex}$  and  $\eta$

$$Z_{ex} = \frac{\int_{\tau_a}^1 \tau^{1/2} d\tau}{\int_{\tau_a}^1 \frac{\tau^{1/2} d\tau}{1 + \eta \langle Z^2 \rangle}} \quad (22)$$

When  $\eta$  is small, an accurate expression for  $\eta$  can be obtained from a Taylor expansion coupled with setting  $\tau_a = 0$ . The result is

$$\eta = \frac{Z_{ex}^2 - 1}{\langle Z^2 \rangle} \quad (23)$$

where

$$\langle Z^2 \rangle = \int_0^1 dx \langle Z^2 \rangle_{x^{2/3} T_0} \quad (24)$$

and the variable of integration  $x = \tau^{3/2}$ . Expression (23), is then substituted into (18b). We can combine (16), (17), (18b), (23), and (24) into a formula for the limiting density  $n_c$  valid when  $Z_e \sim 1$

$$n_c(T_0) = \frac{B_0 c e m^{1/4} (\lambda n \Lambda)^{1/2}}{2\pi R} \left( \frac{1}{Z_{ex} - 1} \right)^{1/2} \frac{1}{\hbar}^{1/2} \quad (25)$$

where

$$\bar{n} = \frac{\langle Z^2 \rangle \tau_c^{3/2} \pi^{3/2}}{(0.582) 2^{5/2} T_0^{3/2} L(\tau_c T_0)} \quad (26)$$

We should keep in mind that  $\tau_c$  differs for the two cases,  $Z_e \gg 1$  and  $Z_e \approx 1$ , because of the different equations [(11), (14), and (15) versus (10), (13), and (15)] used to determine  $\tau_c$ .

We can rewrite our results for the limiting density  $n_c$  as

$$n_c(T_{eo}) = \begin{cases} n_1(T_{eo}) \left(\frac{B}{T}\right) \left(\frac{1m}{R}\right) & Z_e \gg 1 \\ n_2(T_{eo}) \frac{1}{(Z_{ex}-1)^{1/2}} \left(\frac{B}{T}\right) \left(\frac{1m}{R}\right) & Z_e \approx 1 \end{cases} \quad (27a)$$

$$(27b)$$

and use equations (16), (17), and (18a) to evaluate  $n_1$  and (25) and (26) to evaluate  $n_2$ .

Figures 1 and 2 are the principal results of this paper. They show the limiting densities  $n_1$  and  $n_2$  evaluated numerically as a function of assumed central temperature for a variety of common impurity species. It is these figures which demonstrate that this limiting density is remarkably independent of central electron temperature, particularly for experimentally typical values near  $T_0 \approx 1$  keV.

Sensitivity Studies. For an iron impurity, we have evaluated the sensitivity of our limiting densities to two of our assumptions: that the radius of the current carrying channel is determined by  $q = 2$ , and that  $\epsilon = 0.8$  [See Eq. (15)]. Figure 3 gives the limiting densities for various  $q$  and  $\epsilon$  values. The limiting densities are insensitive to modest changes in  $q$  and  $\epsilon$ . Since

increasing  $q$  (the size of the current-carrying channel) decreases the limiting density, the values computed for  $q = 2$  represent an upper limit as desired. Other impurity species are similarly insensitive.

Coronal equilibrium is not an accurate model for the detailed ionization state equilibrium in a tokamak. Impurity transport processes provide radial fluxes of individual ionization states that can compete with the ionization and recombination processes which govern coronal equilibrium.<sup>16</sup> Charge exchange with neutral hydrogen atoms also alters the ionization equilibrium.<sup>17</sup> In both cases, the effect in the central plasma region is to reduce the degree of ionization at a given temperature. This, in turn, increases the impurity radiation rate,<sup>16,17</sup> thereby lowering the maximum density. Therefore, the coronal equilibrium model provides an upper limit to the density, consistent with the objectives of this paper. To investigate the sensitivity of the density limit to deviations from coronal ionization equilibrium in a simple way, we have computed the limiting density from a model in which the coronal ionization equilibrium temperature  $T_q$  is lower than the excitation temperature  $T_{ex} = T_e$  used to compute the radiation rate of the various ionization stages. Figure 4 shows the results for several impurity elements when  $T_q = 0.8 T_e$ . As expected, the limiting densities are lower, but are 80%-90% of the unshifted  $T_q = T_{ex}$  coronal equilibrium model. As tokamak devices become larger, the importance of transport process will decrease relative to ionization and recombination and coronal ionization equilibrium will be more accurate.

Let us summarize our sensitivity studies. Increasing the current channel size (i.e.,  $q > 2$ ) and altering the ionization equilibrium both reduce the maximum density somewhat. Increasing  $\epsilon$  to  $\epsilon = 0.9$  produced a negligible increase in the maximum density. We can therefore conclude that the maximum

densities reported in Figs. 1 and 2 are indeed bonafide upper limits for the central density of all ohmically heated tokamak discharges. To the extent that the density limit is determined by the radiative power balance, these sensitivity studies show that these calculated limits should be meaningfully close to those actually obtained in experiments. We note that our results for iron and other intermediate - z impurities agree well with Murakami's original observations<sup>1</sup>, while our results for low-z impurities such as oxygen are somewhat higher.

Edge Radiation. The radiative cooling rates for most impurities increase towards the low charge states typically found in the cooler edge regions of ohmically heated plasmas, and energy transport from the center of the plasma must supply sufficient power to maintain this edge radiation. Previous studies of the Murakami limit have concentrated on criteria which arise from this relationship.<sup>4-6</sup> We will consider the electron thermal conductivity and cooling in a  $T_e \sim 100$  eV edge plasma to show that a tokamak can generally adjust its central temperature to satisfy the edge radiation criterion provided that the edge electron thermal diffusivity does not exceed the Bohm value.

The paper of Rebut and Green<sup>3</sup> introduced a useful and informative method for analyzing the thermal balance of the edge plasma. A slab model is perfectly satisfactory for the edge plasma so the steady-state electron thermal heat conductivity equation can be written as

$$\frac{d}{dx} \kappa \frac{dT_e}{dx} - n^2 \eta L(T) = 0 \quad . \quad (28)$$

Rebut and Greene pointed out that by multiplying Eq. (28) by  $\kappa(dT_e/dx)$ , one could integrate Eq. (28) to obtain

$$h^2 = \left( \kappa \frac{dT_e}{dx} \right)^2 = 2 \int_0^T n^2 \eta \kappa L(T) dT + h_a^2 \quad (29)$$

where  $h_a$  is the heat flux at the plasma boundary. On the right-hand side of Eq. (29), the spatial dependence of density and thermal conductivity enter implicitly through the temperature profile.

Let us assume that the electron thermal diffusivity is bounded by the Bohm value so that

$$\kappa \leq n \left( \frac{cT}{16eB} \right) \quad (30)$$

The heat flux out of the current-carrying channel must then satisfy the inequality

$$h^2 > \frac{1}{8} (\bar{n})^3 \eta \int_0^T \frac{cT'}{eB} L(T') dT' \quad (31)$$

where  $\bar{n}$  is an average density in the region where  $T L(T)$  has its maximum. The integral  $\int_0^T L(T') dT'$  will be shown to be reasonably independent of our chosen edge region defining temperature  $T \sim 100$  eV. The value of the edge density  $\bar{n}$  is normalized to the central density by the definition

$$\Delta = \frac{\bar{n}}{(n_c)_{T_0 = 1 \text{ keV}}} \quad (32)$$

where  $n_c$  is given by (27a) evaluated at  $T_0 = 1$  keV. One expects that  $\Delta$  will be a small number (i.e.,  $\Delta < 0.2$ ). We note that the relative importance of any edge radiating "shell" region is sensitively dependent on the plasma density profile since radiative cooling is proportional to  $[n_e(r)]^2$  assuming a



constant impurity concentration.

The heat flux flowing out of the current-carrying channel is

$$h = \frac{Q}{2\pi a} = \frac{1-\epsilon}{2a} \frac{j_0^2 b^2}{\sigma_0} \eta \langle Z^2 \rangle_0 \left[ \int_0^1 d\tau' (\tau')^{1/2} \frac{\langle Z^2 \rangle_0}{\langle Z^2 \rangle} \right] \quad (33)$$

Because our interest centers on impure plasmas, formulas appropriate for the  $Z_e \gg 1$  case have been used. The heat flux can be recast, with the help of Eqs. (2) through (5) and (14), into the form

$$h = (1 - \epsilon) \frac{B_T^2 c^2 a \eta \langle Z^2 \rangle_0 m^{1/2} e^2 (\ln \Lambda)}{8\pi^2 R^2 q_L T_0^{3/2}} \left( \frac{\pi^{3/2}}{2^{5/2}} \right) \quad (34)$$

Inequality (31) can then be written as

$$\frac{(1-\epsilon)^2}{\Delta^3} \frac{B_T^5 c^3 a^2 Z_e \langle Z^2 \rangle_0 e^5 m (\ln \Lambda)^2}{256\pi^2 q_L^2 R^4 T_0^3 [n_c^3 \int_0^T T' L(T') dT']} > 1 \quad (35)$$

where we used  $Z_e = \eta \langle Z^2 \rangle_0$ . Apart from the magnetic field and major radius scalings expressed by (27a) the quantity in the [ ] brackets is a property solely of the impurity species. Let us rewrite inequality (35) in practical units. The result is

$$\frac{(1-\epsilon)^2}{\Delta^3} \left( \frac{Z_e a^2}{R^2 q_L} \right) \frac{\langle Z^2 \rangle_0 (B_T/1T)^2 (R/1m)}{(T_0/1\text{keV})^3 \left[ \frac{n_1}{10^2} \int_0^T T' L(T') dT' \right]} > 200 \quad (36)$$

where Table 1 should be used to evaluate the [ ] brackets.

Equation (36) helps illuminate the behavior of the plasma as the density is raised and radiative losses begin to dominate the energy balance. It is the strong variation of  $\langle Z^2 \rangle_0 / T_0^3$  over the range  $100 \text{ eV} < T_0 < 1 \text{ keV}$  that

enables a tokamak discharge to adopt a central electron temperature which satisfies the edge heat flux inequality (36). If the central temperature is forced to drop to an extremely low value before our critical density is approached by the core, the edge region effectively dominates the plasma. Inequality (36) shows that this will tend to occur at low fields, in smaller devices, and with flatter density profiles. For most tokamaks, the edge radiation can be supported by modest adjustments in  $T_0$ , thereby moving consideration of the critical power balance region to the core and the limits reported in Eqs. (27a) and (27b). In all cases, this core-derived limit must be satisfied by the plasma regardless of details of the core-edge relationship.

### 3. THE REVERSED-FIELD PINCH I/N LIMIT

Reversed-field pinch experiments depend on ohmic heating to overcome impurity radiation losses. A high density limit, known as the I/N limit, has been experimentally established and found to agree with a zero-dimensional criterion that the ohmic heating rate exceed the impurity radiation. The review of Ortolani and Rostagni<sup>10</sup> provides an excellent account of these matters.

The objective of this section is to evaluate the I/N limit for variety of potential impurity elements to aid in the selection of materials and in the interpretation of experiments. For definiteness, we shall present a brief derivation of our formula for the I/N limit.

The starting point is the well-known force-free equilibrium for a reversed-field pinch which satisfies the equation

$$\vec{\nabla} \times \vec{B} = \alpha \vec{B} = \frac{4\pi}{c} \vec{j}_0 \quad (37)$$

where  $\alpha$  is a constant. The solution is known to be

$$\hat{B} = B_0 (\hat{z} J_0(\alpha r) + \hat{\theta} J_1(\alpha r)) \quad (38)$$

so that

$$j = \frac{\alpha B_0}{4\pi} (J_0^2 + J_1^2)^{1/2} \quad (39)$$

In contrast to a tokamak where the current density is proportional to the conductivity, the current density in a reversed-field pinch is a prescribed function of radius which satisfies the force-free equilibrium Eq. (37). The Taylor minimum energy principle<sup>19</sup> says that  $\alpha$  must be a constant.

Let us form the ratio  $\Sigma$  of the ohmic heating input to the radiative loss rate

$$\Sigma = \frac{j^2}{\sigma n^2 \eta L(T)} = \frac{j_0^2 (J_0^2 + J_1^2)}{\sigma n_0^2 L(T) [1 - (r^2/a^2)^2]} \quad (40)$$

The spatial dependence of current density and plasma density are essentially the same for a parabolic density profile

$$\frac{j^2}{j_0^2} = (J_0^2 + J_1^2) = 1 - \frac{\alpha^2 r^2}{4} = 1 - \frac{\eta_0^2}{4} \frac{r^2}{a^2} \quad (41)$$

$$\frac{n}{n_0} = \left(1 - \frac{r^2}{a^2}\right)^2 = 1 - \frac{2r^2}{a^2} \quad (42)$$

because  $\alpha = \eta_0/a$  and  $\eta_0 = 2.8 - 3.0$  for reversed-field pinch configurations.

Therefore the principal variation of ratio  $\Sigma$  with radius arises from

temperature variations which are not well-known. Our approach is to find the temperature at which the ratio  $\Sigma$  is a minimum and relate that to the I/N limit.

We can use Ampere's law to relate the central current density to the total current

$$B_{\theta} = B_0 J_1(\alpha a) = \frac{2I}{ca} \quad (43)$$

Substituting from (43) into (39), one finds that the central current density takes the form

$$j_0 = \frac{\alpha I}{2\pi a J_1(\eta_0)} = \frac{I}{\pi a^2} \left( \frac{\eta_0}{2J_1(\eta_0)} \right) \quad (44)$$

The ratio  $\Sigma$  can then be expressed as

$$\Sigma = \frac{I^2}{N^2} \left( \frac{\pi}{5/2} \right)^{3/2} (m^{1/2} e^2 (kT)) \left( \frac{\langle Z^2 \rangle}{T^{3/2} L(T)} \right) \left( \frac{\eta_0}{4J_1(\eta_0)} \right)^2 \quad (45)$$

where the line density N is

$$N = \frac{n_0 \pi a^2}{2} \quad (46)$$

and where the formulas (2) and (4) were used for the conductivity. Again, we use the limit  $Z_e - 1 = \eta \langle Z^2 \rangle \gg 1$  appropriate to plasmas with significant impurity concentrations. In this limit, the ratio of ohmic heating power to impurity radiation becomes independent of the impurity concentration as was noted by Ortolani and Rostagni.<sup>10</sup> Equation (45) can be recast to express I/N in terms of  $\Sigma$

$$\frac{I}{N} = (\Sigma)^{1/2} \Psi(T) \quad (47)$$

where

$$\Psi(T) = \left( \frac{T^{3/2} L(T)}{\langle Z^2 \rangle} \right)^{1/2} \frac{0.52}{m^{1/4} e^{(\ln \Lambda)^{1/2}}} \quad (48)$$

and where the value  $\eta_0 = 2.9$  was adopted to evaluate the numerical factors.

The purpose of our work is to investigate the I/N limit as a function of temperature for various impurity species. Hence we must compute the quantity  $\Psi(T)$  versus temperature and determine its maximum value for each impurity species. The appropriate numerical value of  $\ln \Lambda$  is  $\ln \Lambda = 12$ . The maximum value of  $\Psi(T)$  corresponds to the I/N limit for a reversed-field pinch. Figure 5 shows the results:  $\Psi(T)$  expressed in amps-m for a variety of impurity elements.

#### 4. DISCUSSION

Impurity radiation places an upper limit on the density of ohmically heated tokamak discharges. Our key result is that radiation from the central portion of the tokamak discharge determines this limit. The detailed behavior which leads a radiation-dominated tokamak plasma to disruption at some critical density is beyond the scope of this paper. Our calculation has instead examined the question of the ohmic heating/radiative cooling balance in the critical current-carrying core region of the plasma, and thereby arrives at a firm upper limit to this disruption density. Consideration of the core power balance is more straightforward and reliable than previous studies which focused on the edge region of the plasma. The relevance of our

approach is confirmed by the fact that it yields limits sufficiently low as to be of direct importance in the planning and analysis of typical tokamak experiments.

Our simple single-impurity-species approach shows the important variation of the density limit as the impurity species is changed. Equations (27a) and (27b) and Figs. 1 and 2 summarize the calculations. Most real tokamaks contain mixtures of several impurity species. In this case, our limits will fall between the corresponding curves.

The density limits of Figs. 1 and 2 represent bonafide theoretical upper limits. Additional physics considerations such as increasing the central region beyond the  $q = 2$  surface (Fig. 3) or deviations from coronal ionization equilibrium (Fig. 4) result in somewhat lower density limits. As true constraints, the density limits apply to ohmically heated target plasmas and discharge termination phases in future large plasma devices such as TFTR, JET, or reactors. There are quite evident advantages to eliminating all medium- and high-Z impurity elements should high density target plasmas be desired. Beryllium limiters would permit a target plasma density in excess of  $10^{14} \text{ cm}^{-3}$  for many proposed devices if oxygen, etc. can be effectively removed as well.

Experimentally, tokamak density limits have been found to depend on discharge current as well as  $B_T/R$ . The data are often displayed on "Hugill plots."<sup>20</sup> Our density limits do not depend on current and therefore correspond to the highest density limit observed as the current is varied, i.e., to the maximum value of  $\bar{n}R/B_t$  as  $1/q_L$  is varied on a Hugill plot. The broad maximum occurs near  $q_L = 4$ . Indeed, this is where our approximations should be the best. When  $q_L = 4$ , the  $q = 2$  surface is sufficiently within the plasma so that the surface boundary condition should not alter the electron temperature profile from the Gaussian form assumed. On the other hand, there

is not a large plasma region outside the  $q = 2$  surface which must be maintained by a heat flux from the central region. Quantitatively, our limit agrees with results from DITE,<sup>20</sup> given an oxygen impurity and an appropriate factor (e.g. 0.67) relating central and line - average density.

Let us note that densities  $n_1$  and  $n_2$  have close numerical values. As a general guide, we can use the rough interpolation formula

$$n_M = \left( \frac{n_1 + n_2}{2} \right) \left( \frac{Z}{Z-1} \right)^{1/2} \left( \frac{B_T}{1T} \right) \left( \frac{1m}{R} \right) \quad (49)$$

to express the limiting density succinctly. The values quoted in the abstract are based on Eq. (49).

Radiation from the plasma periphery has been a principal feature in previous treatments of tokamak density limits.<sup>3-6</sup> Our arguments show that peripheral impurity radiation per se often need not be considered in a global radiative power balance derived density limit [see Inequality (36)]. On the other hand, the consequence of exceeding the density limit is to cool the plasma periphery because the ratio of local ohmic heating input to radiative cooling decreases outward in a tokamak. This decrease arises from two physics processes which reinforce each other: higher radiation rates at low temperatures and smaller ohmic heating input because the current density is proportional to the conductivity. Exceeding the density limit simply means that no excess power is available from the plasma center to maintain the edge plasma. As a result the current channel shrinks and a disruption ensues.

The I/N limit in a reversed-field pinch is essentially the same limit as the radiative power balance limit in tokamaks.<sup>10</sup> Our contribution is to evaluate this limit for many impurity species. Figure 5 gives the results. As reversed-field pinch devices turn towards Inconel metallic liners, it is

clear that iron and nickel impurities will form a more formidable radiation barrier in the range  $100 \text{ eV} < T_e < 1 \text{ keV}$ , than did oxygen near  $T_e \sim 30 \text{ eV}$ . Beryllium is again a superior material.

Let us conclude by observing that, while our density limit exhibits the  $E_m/R$  scaling observed by Murakami,<sup>†</sup> the multiplying factor is not universal but has an important dependence on impurity species and concentration. Reducing the impurity concentration obviously increases the density limit, but the improvement is slow according to Eq. (27b). It is more effective to eliminate high-Z impurity species by a judicious choice of limiter material.

#### ACKNOWLEDGMENTS

It is a pleasure to thank Dr. D. E. Post for his interest in this research, and D. R. Mikkelsen for useful discussions. Our work was supported by U.S. Department of Energy Contract No. DE-AC02-76-CHO-3073.



TABLE I. VALUES FOR EDGE RADIATION CRITERION

Impurity		$n_1^3 \int_0^T T' L(T') dT'$		$\langle Z^2 \rangle_0$	
Element	$(10^{13} \text{ cm}^{-3})$	$T = 100 \text{ eV}$	$T = 200 \text{ eV}$	$T_0 = 100 \text{ eV}$	$T_0 = 1 \text{ keV}$
		$(10^2 \text{ erg}^3 \text{ cm}^{-6} \text{ sec}^{-1})$			
Be	12.0	0.45	0.78	16	16
C	7.5	0.76	1.60	28	36
O	5.0	1.20	1.75	37	64
Ti	1.2	0.45	0.90	116	380
Fe	0.9	0.28	0.95	98	410
Mo	0.7	0.16	0.34	165	610
W	0.4	0.04	0.12	165	750

REFERENCES

- <sup>1</sup>M. Murakami, J. D. Callen, and L. A. Berry, Nucl. Fusion **16**, 347 (1976).
- <sup>2</sup>A. Gibson, Nucl. Fusion **16**, 546 (1976).
- <sup>3</sup>P. H. Rebut and B. J. Green, in Plasma Physics and Controlled Nuclear Fusion Research (Proc. 6th International Conference Serchesgaden, 1976) (IAEA, Vienna, 1977), Vol. 2, p. 3.
- <sup>4</sup>D. E. T. F. Ashby and M. H. Hughes, Nucl. Fusion **21**, 911 (1981).
- <sup>5</sup>N. Ohya, Nucl. Fusion **19**, 1491 (1979).
- <sup>6</sup>D. E. Roberts, Nucl. Fusion **21**, 215 (1981); D. E. Roberts, Nucl. Fusion **23**, 311 (1983).
- <sup>7</sup>H. P. Furth, Physica Scr., **T2/2**, 324 (1982).
- <sup>8</sup>P. H. Rebut "JET Joint Undertaking: March 1982" in Proceedings of the Third Joint Varenna-Grenoble International Symposium on Heating in Toroidal Plasmas, Grenoble, 1982, Vol. III, p. 989.
- <sup>9</sup>D. E. Post, R. V. Jensen, C. B. Tarter, W. H. Grossberger, and W. A. Lokke, At. Data Nucl. Data Tables **20**, 397 (1977).
- <sup>10</sup>S. Ortolani and G. Rotagni, Nucl. Instrum. Methods **207**, 35 (1983).
- <sup>11</sup>B. Coppi, Comments Plasma Phys. Cont. Fusion **5**, 261 (1980).
- <sup>12</sup>R. Goldston et al., Heating in Toroidal Plasmas, Proceedings of the 2nd Joint Grenoble-Varenna Symposium, Como, Italy, 1980, Vol. II, p. 711. See Fig. 9.
- <sup>13</sup>R. J. Fonck and R. A. Hulse, Princeton Plasma Physics Laboratory Report PPPL-2068, December, 1983; (to be published).
- <sup>14</sup>R. M. More, Lawrence Livermore Laboratory Report UCRL-84991, March, 1981.
- <sup>15</sup>L. Spitzer, Physics of Fully Ionized Gases, (Interscience, New York, 1962) p. 139.

- 16 R. A. Hulse, Nucl. Technol./Fusion 3, 259 (1983).
- 17 R. A. Hulse, D. E. Post, and D. R. Mikkelsen, J. Phys. B13, 3895 (1980).
- 18 L. A. Berry et al., in Plasma Physics and Controlled Nuclear Fusion Research (Proc. 6<sup>th</sup> International Conference Berchtesgaden, 1976), (IAEA, Vienna, 1977), Vol. 1, 49.
- 19 J. B. Taylor, Phys. Rev. Letters 33, 1739 (1974).
- 20 K. B. Axon et al., in Plasma Physics and Controlled Nuclear Fusion Research (Proc. 8th International Conference Brussels, 1980), (IAEA, Vienna, 1981), Vol. 1, 413. See Fig. 7.

FIGURE CAPTIONS

FIG. 1. Central electron density  $n_1$  to be used in Eq. (27a).

FIG. 2. Central electron density  $n_2$  to be used in Eq. (27b).

FIG. 3 (a) Sensitivity of the density  $n_2$  to changes in the current-channel size (q-value) and to the value of  $\epsilon$  for an iron impurity. Solid curves are for  $\epsilon = 0.8$  and the dashed curves for  $\epsilon = 0.9$ . (b) Sensitivity of the density  $n_1$  to changes in the current channel size (q-value) and to the value of  $\epsilon$  for an iron impurity. Solid curves are for  $\epsilon = 0.8$  and the dashed curves for  $\epsilon = 0.9$ .

FIG. 4. Sensitivity of the limiting density  $n_1$  to deviations from coronal equilibrium for various impurity elements.  $T_q$  denotes the temperature governing coronal ionization equilibrium and  $T_{ex} = T_e$  the temperature governing radiation rates from a given ionization equilibrium.

FIG. 5. Zero-dimensional I/N limit,  $\Psi(T)$ , for a reversed-field-pinch for a variety of impurity elements.

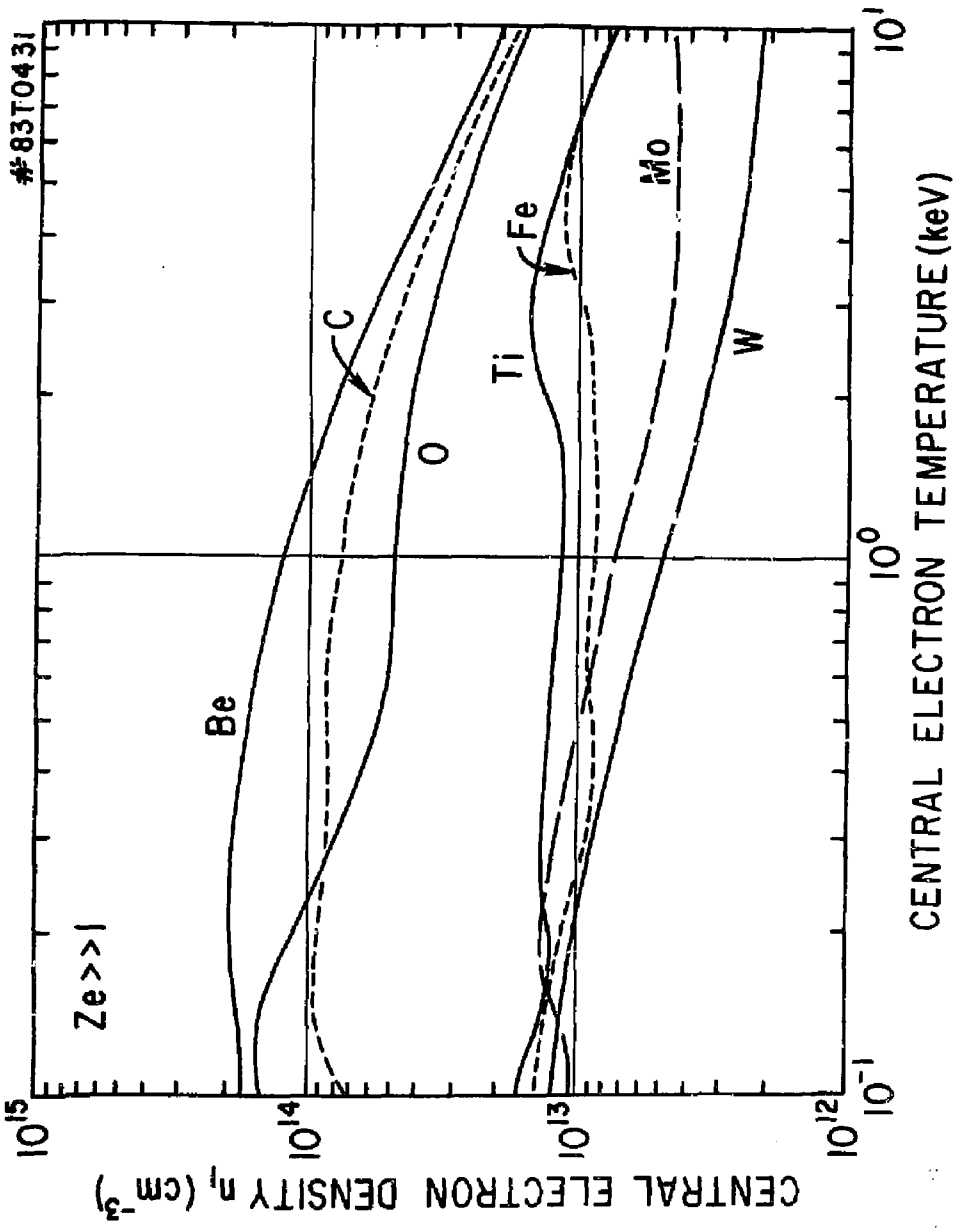


Fig. 1

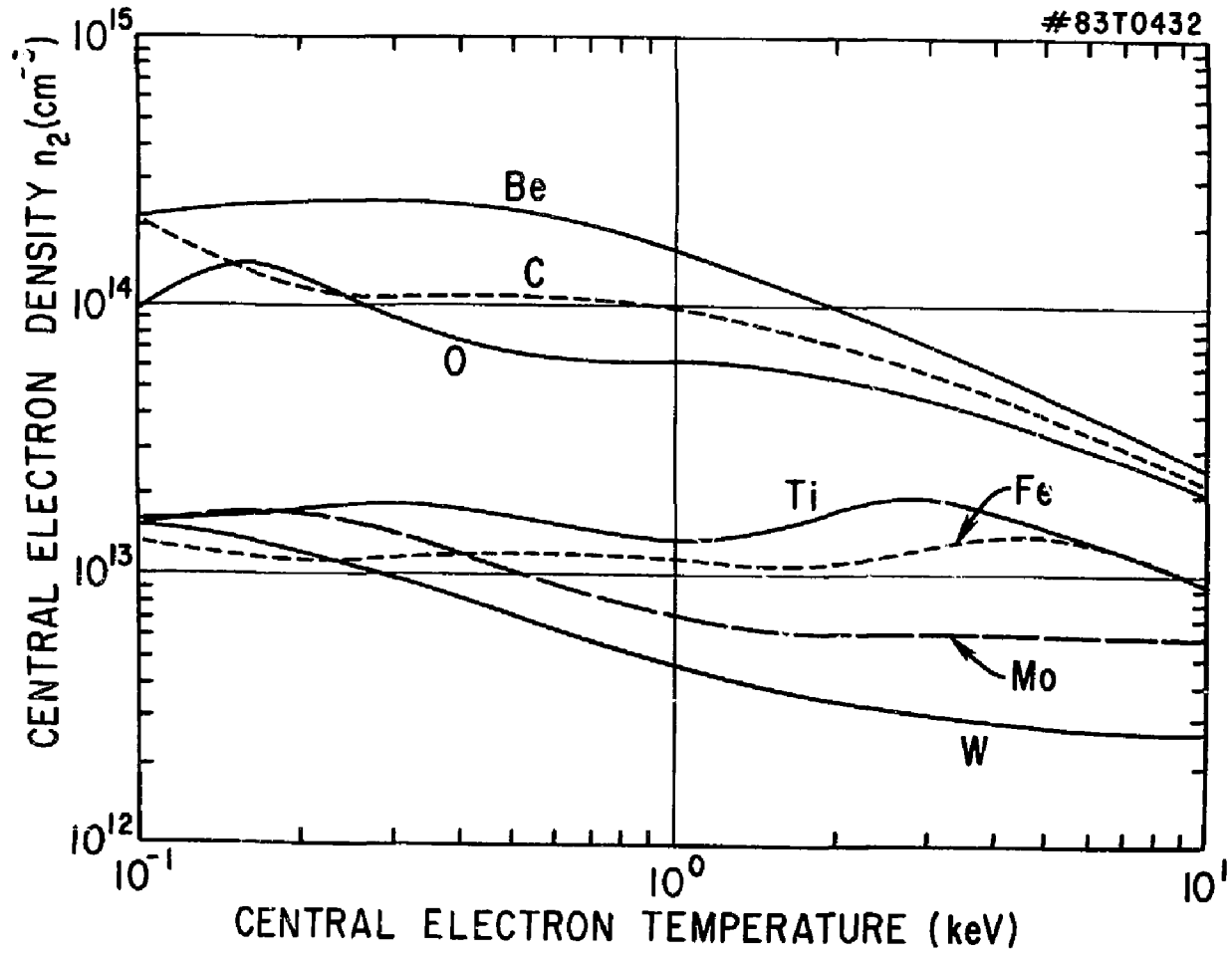


Fig. 2

#83T0433

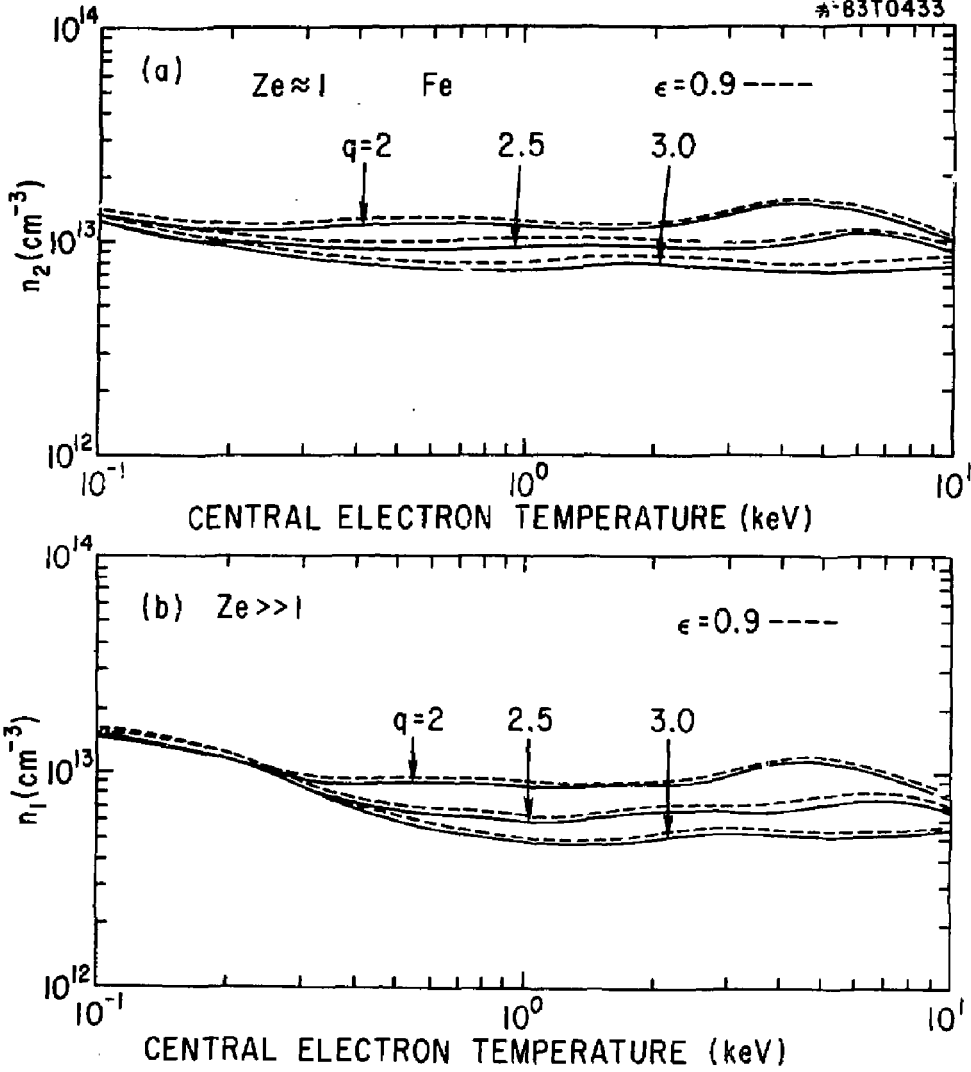


Fig. 3

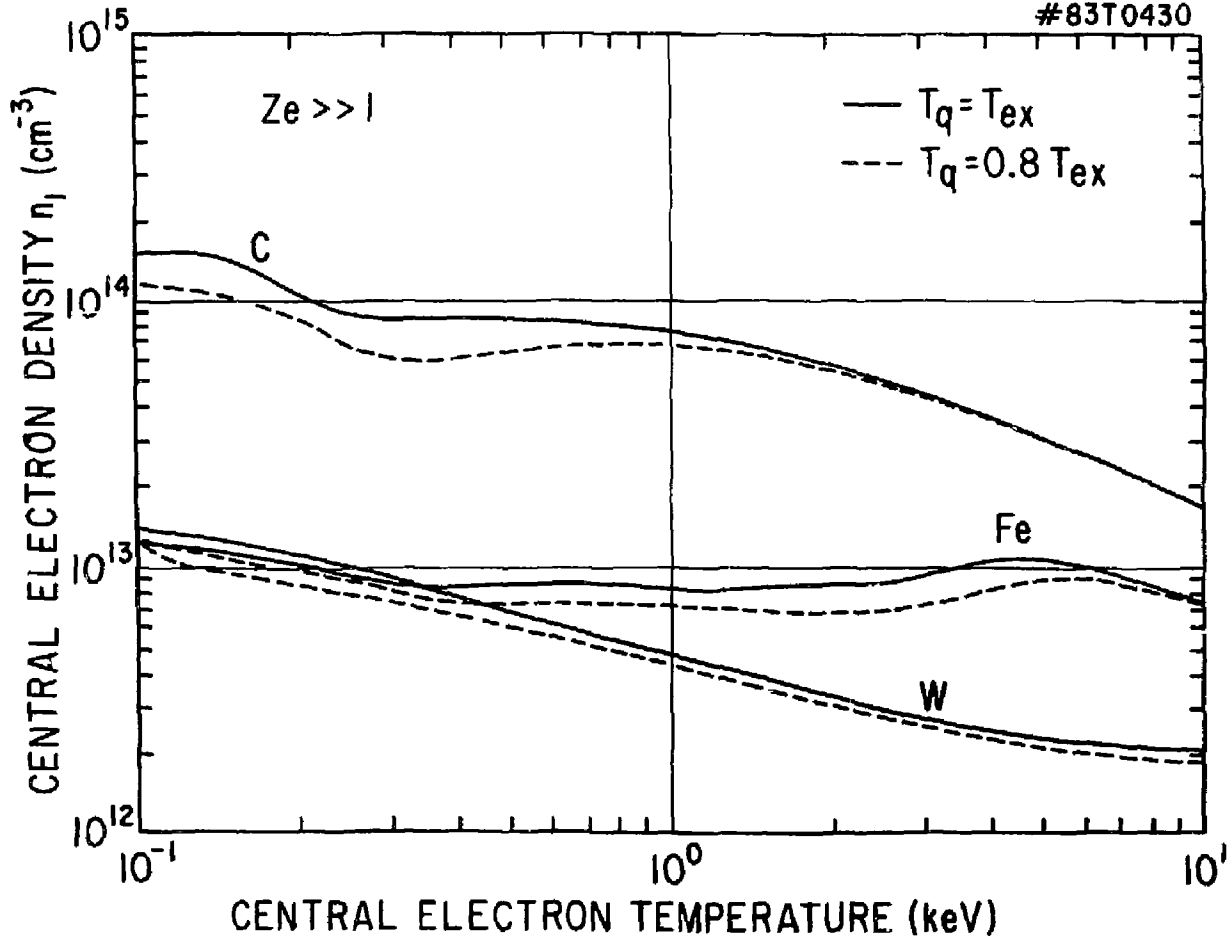


Fig. 4



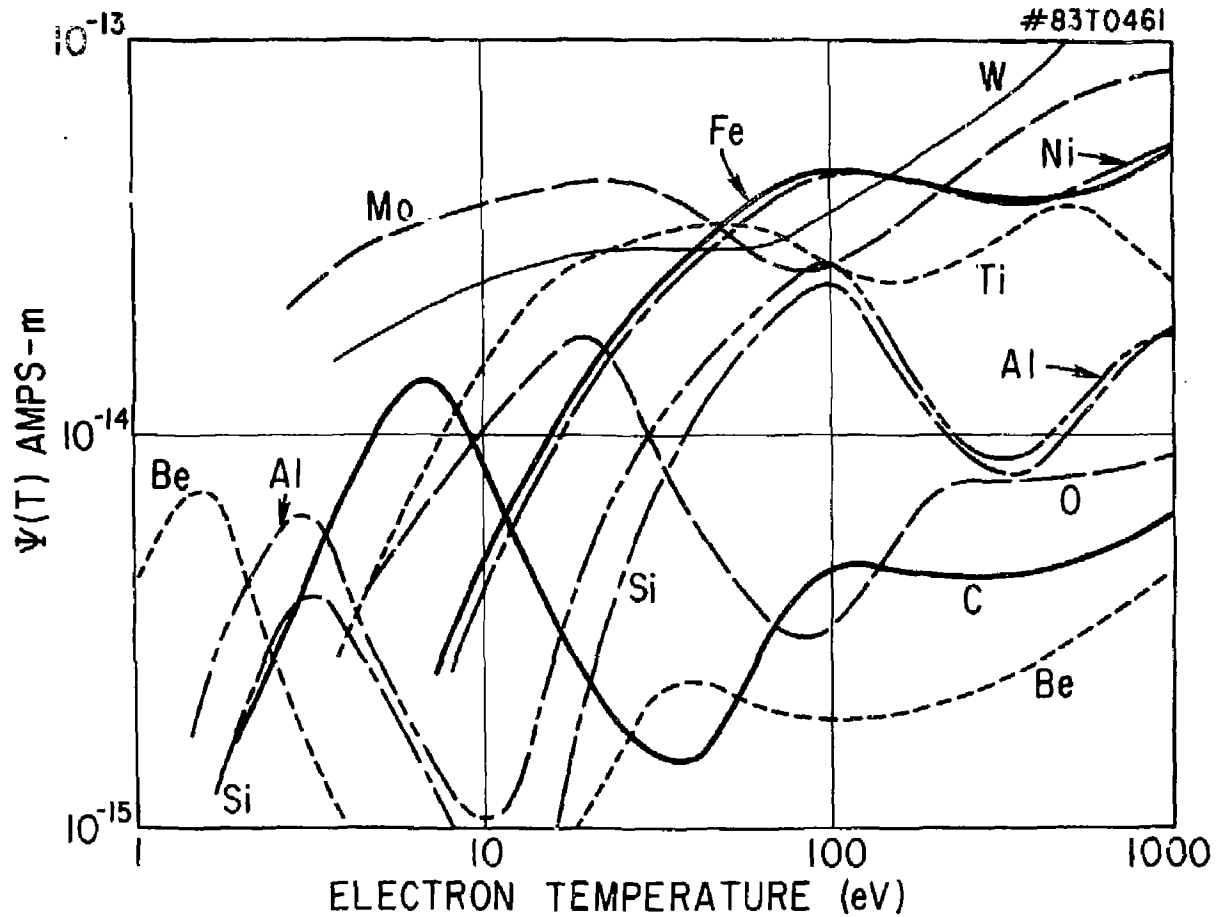


Fig. 5

EXTERNAL DISYRIBUTION IN ADDITION TO TIC UC-20.

Fisika Res Lab, Austr Nat'l Univ, AUSTRALIA  
Dr. Frank J. Paoloni, Univ of Wollongong, AUSTRALIA  
Prof. I.R. Jones, Flinders Univ., AUSTRALIA  
Prof. M.J. Brennan, Univ Sydney, AUSTRALIA  
Prof. F. Cop, Inst Theo Phys, AUSTRIA  
Prof. Frank Verheest, Inst theoretische, BELGIUM  
Dr. D. Palumbo, Dg XII Fusion Prog, BELGIUM  
Ecole Royale Militaire, Lab de Phys Plasmas, BELGIUM  
Dr. P.H. Sakaneke, Univ Estadual, BRAZIL  
Dr. C.R. James, Univ of Alberta, CANADA  
Prof. J. Teichmann, Univ of Montreal, CANADA  
Dr. H.M. Skarsgard, Univ of Saskatchewan, CANADA  
Prof. S.R. Sreenivasan, University of Calgary, CANADA  
Prof. Tudor W. Johnston, INRS-Energie, CANADA  
Dr. Hennes Barnard, Univ British Columbia, CANADA  
Dr. M.P. Bachynski, MPB Technologies, Inc., CANADA  
Zhengou Li, SW Inst Physics, CHINA  
Library, Tsing Hua University, CHINA  
Librarian, Institute of Physics, CHINA  
Inst Plasma Phys, Academia Sinica, CHINA  
Dr. Peter Lukac, Komenského Univ, CZECHOSLOVAKIA  
The Librarian, Culham Laboratory, ENGLAND  
Prof. Schatzman, Observatoire de Nice, FRANCE  
J. Radet, CEN-CE6, FRANCE  
AM Dupas Library, AM Dupas Library, FRANCE  
Dr. Tom Muoi, Academy Bibliographic, HONG KONG  
Preprint Library, Cent Res Inst Phys, HUNGARY  
Dr. S.K. Trehan, Panjab University, INDIA  
Dr. Indra, Mohan Lal Das, Banaras Hindu Univ, INDIA  
Dr. L.K. Chevda, South Gujarat Univ, INDIA  
Dr. R.K. Chhajlani, Var Ruchi Marg, INDIA  
P. Kaw, Physical Research Lab, INDIA  
Dr. Phillip Rosenau, Israel Inst Tech, ISRAEL  
Prof. S. Cupperman, Tel Aviv University, ISRAEL  
Prof. G. Rostagni, Univ DI Padova, ITALY  
Librarian, Int'l Ctr Theo Phys, ITALY  
Miss Giolla De Palo, Assoc EURATOM-CNEN, ITALY  
Biblioteca, del CNR EURATOM, ITALY  
Dr. H. Yamato, Toshiba Res & Dev, JAPAN  
Prof. M. Yoshikawa, JAERI, Tokai Res Est, JAPAN  
Prof. T. Uchida, University of Tokyo, JAPAN  
Research Info Center, Nagoya University, JAPAN  
Prof. Kyoji Nishikawa, Univ of Hiroshima, JAPAN  
Prof. Sigeru Mori, JAERI, JAPAN  
Library, Kyoto University, JAPAN  
Prof. Ichiro Kawakami, Nihon Univ, JAPAN  
Prof. Setoshi Itoh, Kyushu University, JAPAN  
Tech Info Division, Korea Atomic Energy, KOREA  
Dr. R. England, Ciudad Universitaria, MEXICO  
Bibliothek, Fom-Inst Voor Plasma, NETHERLANDS  
Prof. B.S. Liley, University of Waikato, NEW ZEALAND  
Dr. Suresh C. Sharma, Univ of Calabar, NIGERIA  
Prof. J.A.C. Cabral, Inst Superior Tech, PORTUGAL  
Dr. Octavian Petrus, ALI CUZA University, ROMANIA  
Prof. M.A. Hellberg, University of Natal, SO AFRICA  
Dr. Johan de Villiers, Atomic Energy Bd, SO AFRICA  
Fusion Div. Library, JEN, SPAIN  
Prof. Hans Wilhelmson, Chalmers Univ Tech, SWEDEN  
Dr. Lennart Stenflo, University of UMEA, SWEDEN  
Library, Royal Inst Tech, SWEDEN  
Dr. Erik T. Karlson, Uppsala Universitet, SWEDEN  
Centre de Recherches, Ecole Polytech Fed, SWITZERLAND  
Dr. W.L. Weise, Nat'l Bur Stand, USA  
Dr. W.M. Stacey, Georg Inst Tech, USA  
Dr. S.T. Wu, Univ Alabama, USA  
Prof. Norman L. Dixon, Univ S Florida, USA  
Dr. Benjamin Ma, Iowa State Univ, USA  
Prof. Magne Kristiansen, Texas Tech Univ, USA  
Dr. Raymond Askew, Auburn Univ, USA  
Dr. V.T. ToLst, Kharkov Phys Tech Ins, USSR  
Dr. D.D. Ryutov, Siberian Acad Sci, USSR  
Dr. G.A. Eliseev, Kurchatov Institute, USSR  
Dr. V.A. Glukhikh, Inst Electro-Physical, USSR  
Institute Gen, Physics, USSR  
Prof. T.J. Boyd, Univ College N Wales, WALES  
Dr. K. Schindler, Ruhr Universitat, W. GERMANY  
Nuclear Res Estab, Julich Ltd, W. GERMANY  
Librarian, Max-Planck Institut, W. GERMANY  
Dr. H.J. Kaeppeler, University Stuttgart, W. GERMANY  
Bibliothek, Inst Plasmeforschung, W. GERMANY